

Beyond the Light-Cone Propagation of Relativistic Wavefunctions: Numerical Results

Xabier Gutierrez de la Ca ¹ and Alex Matzkin ^{2,*}¹ Departamento de Química-Física, Universidad del País Vasco, UPV/EHU, 48940 Leioa, Spain² Laboratoire de Physique Théorique et Modélisation, CNRS Unité 8089, CY Cergy Paris Université, 95302 Cergy-Pontoise, France

* Correspondence: alexandre.matzkin@u-cergy.fr

Abstract: It is known that relativistic wavefunctions formally propagate beyond the light cone when the propagator is limited to the positive energy sector. By construction, this is the case for solutions of the Salpeter (or relativistic Schrödinger) equation or for Klein–Gordon and Dirac wavefunctions defined in the Foldy–Wouthuysen representation. In this work, we quantitatively investigate the degree of non-causality for free propagation for different types of wavepackets that all initially have a compact spatial support. In the studied examples, we find that non-causality appears as a small transient effect that can in most cases be neglected. We display several numerical results and discuss the fundamental and practical consequences of our findings concerning this peculiar dynamical feature.

Keywords: relativistic quantum mechanics; causality; locality; relativistic Schrödinger equation; Klein-Gordon equation; Dirac equation

1. Introduction

In classical relativistic physics, causality is associated with the light-cone structure of Minkowski space-time: no event can be affected by an event lying outside its past light-cone. In relativistic quantum mechanics, the situation is more involved. It is indeed well-known that a relativistic evolution driven by a positive energy Hamiltonian instantaneously turns an initial state having compact spatial support into a distribution having mathematically a non-zero amplitude everywhere in space [1–3]. Relativistic propagators restricted to the positive energy sector spill outside the light cone [4]: it is only by including the contribution of the anti-particle sector that a causal propagator is obtained.

While this observation points to the necessity of having antiparticles in a relativistic quantum theory in order to preserve causality [5], there are instances in which no negative energies appear. For instance, in the Salpeter equation [6] (also known as the relativistic Schrödinger equation), by construction the propagator is restricted to positive energies. This also appears when the solutions of the Klein–Gordon or Dirac equations are unitarily transformed in the Foldy–Wouthuysen (FW) representation. Given the importance of the FW solutions—they are necessary to obtain the classical limit, and it is sometimes claimed that densities constructed from the FW wavefunctions are the only ones having a physical meaning [7]—it is instructive to investigate to which extent there is an effective propagation outside the light cone. Indeed, the instantaneous spreading of an initially localized wavefunction is a mathematical fact, but it is often regarded as being physically irrelevant on the ground that beyond the light-cone, propagation is extremely small and not detectable in practice for any realistic physical state [8,9].

In this work, we will numerically investigate the fraction of the wavefunction that effectively propagates outside the light-cone for different initial states characterized by different parameters (width, mean momentum, and shape). The common feature to the initial states we will employ is the requirement that they have a compact spatial support.



Citation: Gutierrez de la Ca, X.; Matzkin, A. Beyond the Light-Cone Propagation of Relativistic Wavefunctions: Numerical Results. *Dynamics* **2023**, *3*, 60–70. <https://doi.org/10.3390/dynamics3010005>

Academic Editor: Christos Volos

Received: 15 December 2022

Revised: 24 January 2023

Accepted: 30 January 2023

Published: 6 February 2023



Copyright: © 2023 by the authors. Licensee MDPI, Basel, Switzerland. This article is an open access article distributed under the terms and conditions of the Creative Commons Attribution (CC BY) license (<https://creativecommons.org/licenses/by/4.0/>).

Up to now, most works that have investigated this type of propagation, essentially in the context of the Salpeter equation, have used states that have tails at $t = 0$, such as initial Bessel functions [10] (one of the few cases for which analytical solutions can be obtained) or Gaussian wavepackets [8,11–13]. If the states have initial compact support, we can meaningfully and numerically follow the fraction that remains inside the light cone as time evolves. We will see that although the fraction spilling outside the light cone is small and does so during very short times, it could have observational consequences for elementary particles.

To this end, we will first (in Section 2) set the context by recalling in which situations one is led to deal only with the propagator of the positive energy sector. We will briefly recall in Section 3 the arguments proving the propagator is non-causal. We will give our results in Section 4, describing the method employed and our choice of initial states. We close the paper with a short discussion and conclusive comments (Section 5).

2. Positive Energy Propagation

2.1. Standard Relativistic Wave Equations

The standard relativistic wave equations for spin-0 and spin-1/2 particles, respectively, are the Klein–Gordon (KG) and Dirac equations,

$$i\hbar\partial_t\Phi = H\Phi \tag{1}$$

where H represents the KG or Dirac Hamiltonians

$$H_{KG} = -\frac{\hbar^2}{2m}(\sigma_3 + i\sigma_2)\partial_x^2 + mc^2\sigma_3, \tag{2}$$

$$H_D = -i\hbar c\sigma_1\partial_x + mc^2\sigma_3 \tag{3}$$

and σ_i are the usual Pauli matrices. We have used the Hamiltonian form [14] of the Klein–Gordon equation, for which Φ has two components. We will be interested throughout this work in free propagation along a single spatial direction; therefore, effectively restricting the Hamiltonian to a spatial 1D problem: in this case, the Dirac spinor Φ has only two nontrivial components, and this is why H_D as given by Equation (3) is two dimensional rather than four.

As is well-known [14], both H_{KG} and H_D admit positive and negative energy solutions denoted $\Phi_p^\pm(t, x)$, with the + and – signs corresponding to positive and negative energy solutions. For instance, for the Klein–Gordon equation we have [15]

$$\Phi_p^\pm(t, x) = \frac{1}{2\sqrt{m^2c^4 + p^2c^2}} \begin{pmatrix} mc^2 \pm E_p \\ mc^2 \mp E_p \end{pmatrix} e^{ipx/\hbar} e^{\mp iE_p t/\hbar}, \tag{4}$$

where

$$E_p = \sqrt{m^2c^4 + p^2c^2} \tag{5}$$

and the prefactor is a normalization constant. The propagator $K(t, t'; x, x')$, evolving an initial state $\Phi(t', x')$ into $\Phi(t, x)$, when expanded over the Hamiltonian eigenfunctions will contain contributions from both the positive and negative states $\Phi_p^\pm(t, x)$. It is well-known [4] that while the propagator is causal, $-K(t, t'; x, x')$ vanishes for space-like separated points, for which $x - x' > c(t - t')$; the restrictions $K^\pm(t, t'; x, x')$ to an expansion over the sole positive or negative energy eigenstates are not causal, in the sense that $K^\pm(t, t'; x, x')$ does not vanish for space-like separated events. This is why it is often remarked that negative energies are necessary in order to preserve relativistic causality [5].

2.2. The Salpeter or Relativistic Schrödinger Equation

The Salpeter equation [16], also known as the relativistic Schrödinger equation or the Newton–Wigner–Foldy equation [6,17], describes a spinless particle obeying Equation (1) with a Hamiltonian defined by

$$H_S = \sqrt{-\hbar^2 c^2 \partial_x^2 + m^2 c^4}. \quad (6)$$

Note that although this equation is obtained by formally quantizing the classical relativistic energy, the Salpeter equation was derived in [16] in a particular setting (see [18] for more details). Due to the ambiguities of dealing with the differential inside the square root operator, it is customary to work in momentum space since

$$\sqrt{-\hbar^2 c^2 \partial_x^2 + m^2 c^4} \psi(t, x) = \frac{1}{\sqrt{2\pi\hbar}} \int dp E_p e^{ipx/\hbar} \psi(t, p). \quad (7)$$

The plane-waves of positive energy E_p

$$\psi_p(t, x) = \exp(-ipx/\hbar - iE_p t/\hbar) \quad (8)$$

fulfill the relativistic Schrödinger equation. By definition, H_S is positive definite so that the time evolution only includes a propagator expanded over energy eigenstates, given by Equation (16) below.

Note that an arbitrary initial wavefunction has a Fourier transform

$$\psi(0, x) = \frac{1}{\sqrt{2\pi\hbar}} \int dp e^{ipx/\hbar} \psi(0, p). \quad (9)$$

By solving the evolution in momentum space, the time-evolved spatial wavefunction is formally obtained as the Fourier transform

$$\psi(t, x) = \frac{1}{\sqrt{2\pi\hbar}} \int dp e^{ipx/\hbar} e^{-iE_p t/\hbar} \psi(0, p). \quad (10)$$

2.3. Foldy–Wouthuysen Density for the Klein–Gordon or Dirac Equation

The solutions $\Phi_p^\pm(t, x)$ of the KG or Dirac equation in the canonical representation (2) and (3) are well-known to give rise to apparently curious properties (for example, the eigenvalues of the velocity are always zero in the KG case and c in the Dirac case [14]; or, the classical limit cannot be obtained as $\hbar \rightarrow 0$ [7]). This is due to the fact that particle and anti-particle contributions interfere even in the free case. The Foldy–Wouthuysen transformation [19,20] is a unitary transformation in momentum space that separates particles from anti-particles. For example, in the KG case the (pseudo-unitary) operator

$$U = \frac{(mc^2 + E_p) - \sigma_1 (mc^2 - E_p)}{\sqrt{4mc^2 E_p}} \quad (11)$$

applied to the eigenstates Φ_p^\pm given by Equation (4) lead to

$$\Psi^+(t, p) = U\Phi^+ = \begin{pmatrix} 1 \\ 0 \end{pmatrix} e^{-i(E_p t - px)/\hbar} \quad (12)$$

$$\Psi^-(t, p) = U\Phi^- = \begin{pmatrix} 0 \\ 1 \end{pmatrix} e^{i(E_p t - px)/\hbar} \quad (13)$$

and the transformed Hamiltonian is

$$H_{FW} = UHU^{-1} = \sigma_3 \sqrt{p^2 c^2 + m^2 c^4}. \tag{14}$$

Similar relations for the Dirac solutions may be found in textbooks [14,15].

The solutions Ψ^\pm are indeed uncoupled: an initial particle state $\Psi(0, x) = (\psi(0, x), 0)$ has only an expansion over the $\Psi^+(t, p)$ basis states, and thus only the upper component is non-zero. Note that the H_{FW} Hamiltonian is block diagonal, with each block consisting of a Salpeter equation. We therefore see that if a density is defined from the wavefunctions $\Psi(t, x)$ in the FW representation, then the density of a positive energy state will be simply given by $|\psi(t, x)|^2$, which is precisely the density computed from the Salpeter equation. We stress, however, that such a step involves defining a new density that is different from the standard KG or Dirac densities (a unitary transformation does not change the density nor the current). This new density is free from the issues caused by the fact that the standard KG or Dirac densities mix particles and anti-particles. For this reason, this density displays several advantages and has been favored in some works [7,8,17,21], though it suffers from one important drawback: it is formally non-causal.

3. Non-Causality and Its Physical Implications

3.1. Non-Causality of the Propagator

The most straightforward way for showing the non-causality of the positive energy propagator $K^S(t, t'; x, x')$ associated with the Salpeter Hamiltonian (6), or equivalently the positive component of Equation (14), is to compute its expression. Indeed, by definition the propagator should obey

$$\psi(t, x) = \int dx' K^S(t, t'; x, x') \psi(0, x'). \tag{15}$$

Starting from Equation (10) and using the inverse transform of Equation (9), we immediately obtain

$$K^S(t - t'; x - x') = \frac{1}{2\pi\hbar} \int dp e^{ip(x-x')/\hbar} e^{-iE_p(t-t')/\hbar}. \tag{16}$$

Different methods (see, e.g., [11,22]) lead to the closed-form expression

$$K^S(t - t'; x - x') = \frac{im(t - t')}{\pi\hbar \left((x - x')^2 - c^2(t - t')^2 \right)^{1/2}} K_1 \left[mc \left((x - x')^2 - c^2(t - t')^2 \right)^{1/2} / \hbar \right] \tag{17}$$

where K_1 is a modified Bessel function of the second kind. From the asymptotic behavior $K_1(X) \sim \exp(-X) / \sqrt{X}$ for large X , it immediately follows that the propagator spills beyond the light cone. Recall that K^S , sometimes known as the Newton-Wigner propagator [23], is not Lorentz-invariant but does propagate the wavefunction, Equation (15), whereas a Lorentz-invariant propagator does not [5]. Note that the negative energy propagator displays the same behavior as K^S , with the value for space-like arguments being of opposite sign.

Another line of reasoning relies on Paley-Wiener arguments. It can be proved (see, e.g., [1-3]) that for any semi-bounded Hamiltonian, a wavefunction initially localized on a compact support immediately spreads everywhere as soon as the evolution starts (or, conversely, any wavefunction that remains bounded on a compact support must be zero everywhere). Instructive illustrations of this theorem for simple wave equations were given in Ref. [24].

3.2. Physicality of Positive Energy Propagation

The Salpeter equation, although it is attractive as it results from quantizing the classical relativistic Hamiltonian, is usually regarded as an approximate model for a spinless particle, correctly described by the Klein–Gordon equation. Note, however, that for a neutral particle, the solutions of the Klein–Gordon equation are real and can be combined to obtain a complex wavefunction obeying the Salpeter equation [25,26].

The situation is more involved from the point of view of the FW representation. The interpretational difficulties of the standard KG or Dirac densities are related to the problems of defining a position operator. The position operator \hat{X} in the FW representation is equivalent to the Newton-Wigner position operator [23] in the standard representation. On this basis, it is often argued that the FW density is the physical one [27]. The problem is then knowing how to cope with the non-causal nature of the propagation.

The answer that has been given is, in a nutshell, that non-causality is in practice undetectable. First, it has been argued that the probability of such a detection is so low that it would be unlikely to detect such an event even over billions of years [9]. Second, it is difficult to imagine how signals could be sent superluminally since modulations cannot be produced from the exponentially decaying tail [8]. It can also be remarked that since non-causality is non-negligible only on distances of the order of a Compton wavelength ($\lambda_c = \hbar/mc$) away from the light cone, a detection on this scale is hardly feasible for elementary particles and totally impossible for larger (not to mention macroscopic) bodies, for which the Compton wavelength falls below the Planck length. The first step in assessing whether these observations are plausible is to quantitatively compute the fraction of the wavepacket that is propagated beyond the light cone.

4. Results

4.1. Method

The initial wave packet (WP) is defined by Equation (9), which we rewrite here as

$$\psi(0, x) = \frac{1}{\sqrt{2\pi\hbar}} \int dp e^{ipx/\hbar} C(p; x_0, p_0) \tag{18}$$

where x_0 and p_0 are the average position and momentum, respectively, of our initial wave packet. We require $\psi(0, x)$ to have compact spatial support. In this work, we will set $x_0 = 0$ and consider three different initial WP of the form

$$\psi_f(0, x) = (\theta(\pi\Delta_x/2 - x) - \theta(x - \pi\Delta_x/2)) e^{-ip_0x} f(x) \tag{19}$$

with $f(x)$ given by $\cos^8(x/\Delta_x)$, $\cos^2(x/\Delta_x)$, or 1 (yielding a rectangular distribution). Δ_x gives the scale of the spatial width of the packet, and $\theta(x)$ is the unit step function. $\psi(0, x)$ is normalized to 1.

The initial momentum distribution is computed as the Fourier transform of the compact wave function in coordinate space

$$C_f(p; x_0, p_0) = \frac{1}{\sqrt{2\pi\hbar}} \int_{-\Delta_x\pi/2}^{\Delta_x\pi/2} \psi_f(0, x) e^{-ipx} dx \tag{20}$$

hence, with the present notation, the time evolved wavefunction is given by

$$\psi_f(t, x) = \int dx' K^S(t, t'; x, x') \psi_f(0, x') \tag{21}$$

$$= \frac{1}{\sqrt{2\pi\hbar}} \int dp e^{ipx/\hbar} e^{-iE_p t/\hbar} C_f(p; x_0, p_0). \tag{22}$$

The initial momentum space wavefunctions $C_f(p; x_0, p_0)$ can be obtained analytically,

$$C_{\cos^m}(p; x_0, p_0) = (2m!/\Delta_x^m) \frac{\sin[(p - p_0)\Delta_x\pi/2] \exp[i(p - p_0)x_0]}{(p - p_0) \prod_{n=1}^{m/2} (p - p_0 - \frac{2n}{\Delta_x})(p - p_0 + \frac{2n}{\Delta_x})}, \quad (23)$$

when the initial state is a cosine function, and

$$C_1(p; x_0, p_0) = \frac{2 \sin[(p - p_0)\Delta_x\pi/2]}{p - p_0} e^{i(p - p_0)x_0} \quad (24)$$

for the case of the rectangular distribution for which $f(x) = 1$. Note that the simple poles appearing in the denominator are cancelled out by the sine in the numerator.

In practice, Equation (21) is obtained numerically employing the trapezoidal method in Matlab, with the bounds on the integration variable, p_i and p_f , taken large enough so that $C(p_{i,f}; x_0, p_0) \sim 0$. Numerically, the actual computed value of the wave packet will not be exactly zero outside its compact support (including at $t = 0$), but a very small number that should be smaller than our numerical zero, see Figure 1 for the $f(x) = \cos^8(x/\Delta_x)$ case for which the numerical zero is set at 10^{-20} . The calculations based on the method employed here have recently been compared [28–30] to direct solutions of the relativistic wave equations obtained by employing a high-precision finite-difference scheme, resulting in an excellent agreement. In this section, all our results will be given in natural units, $\hbar = c = m = 1$; hence, the Compton wavelength is $\lambda_C = \hbar/mc = 1$.

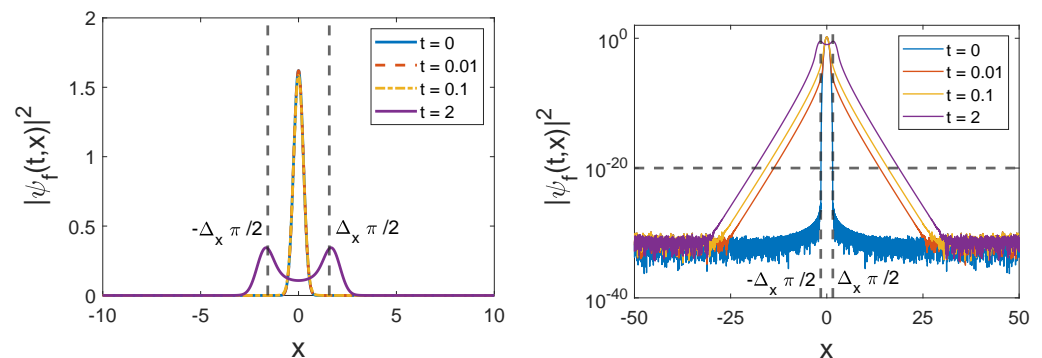


Figure 1. $|\psi_f(t, x)|^2$ for the function with compact support $f(x) = \cos^8(x/\Delta_x)$ (with $\Delta_x = 1$ and $p_0 = 0$) is shown for different values of t (in natural units $\hbar = c = m = 1$). **Left** panel displays the plots in the usual (linear) scale and the **right** panel shows the same quantities with a logarithmic scale. The horizontal dashed line indicates the numerical zero. The initial wavefunction has compact support (no density above the numerical zero), whereas beyond the light-cone propagation appears for times $t > 0$.

4.2. Numerical Results

The left panel of Figure 1 shows the probability density for a typical initial wavefunction with compact support ($\psi_f(0, x)$ is given by Equation (19) with $f(x) = \cos^8(x/\Delta_x)$), along with a few snapshots as the wavefunction evolves. On this scale, the tails propagating outside the light cone are not visible, so we have plotted on the right panel the same quantities on a logarithmic scale, clearly displaying beyond the light-cone propagation (the light cone position is $\pm(\pi/2 + t)$ in these units). Figure 2 (left) shows a density plot for the same initial wavefunction, while the right panel shows the fraction of the density lying outside the light cone as time evolves. This fraction reaches a maximum a very short time after initial propagation and then decreases to zero for longer times. Figure 3 shows the fraction of the probability density outside the light cone for the same $\psi_f(0, x)$ but with different initial widths Δ_x and initial momenta p_0 .

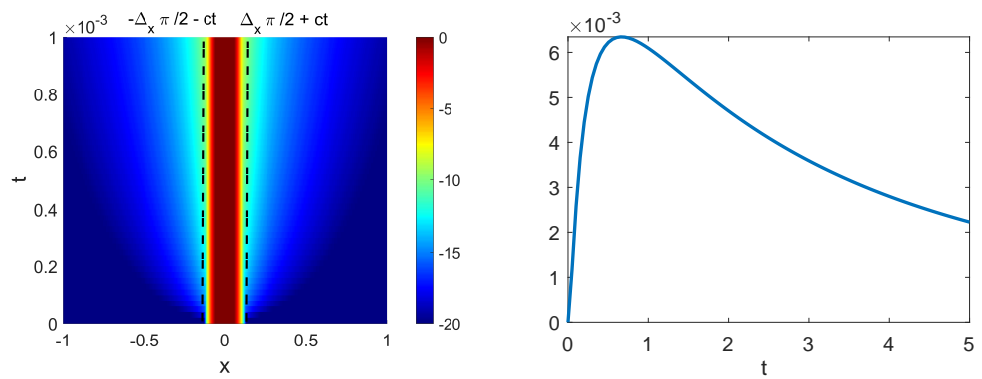


Figure 2. Left panel: time evolution of $\log[|\psi_f(t, x)|^2]$ for the function with initial compact support $f(x) = \cos^8(x/\Delta_x)$ (with $\Delta_x = 1$ and $p_0 = 0$) for short values of t . Note that the tails propagating beyond the light cone appear as soon as $t > 0$. Right panel: Fraction of that same wave packet outside the light cone, where the transient aspect can be noticed.

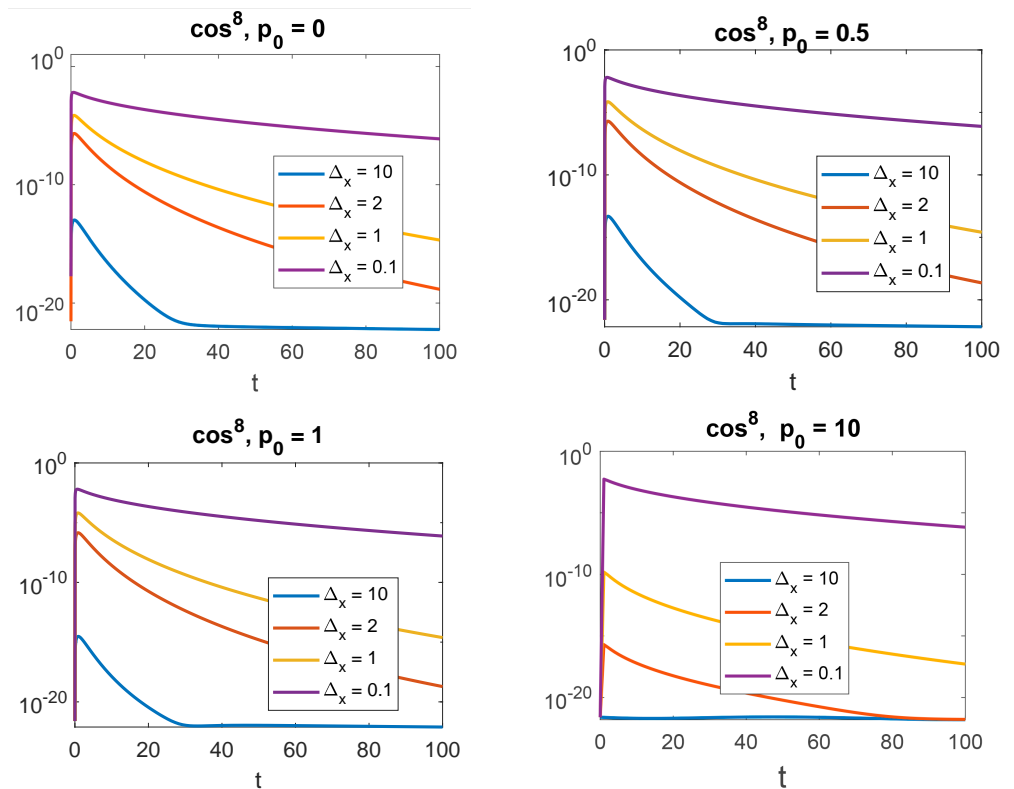


Figure 3. Fraction of the probability density lying outside the light cone for an initial wavepacket $\psi(0, x)$ [Equation (19)] with $f(x) = \cos^8 x/\Delta_x$, where Δ_x and p_0 vary as indicated.

Figures 4 and 5 display similar results but for an initial wavefunction $\psi_f(0, x)$ with $f(x) = \cos^2(x/\Delta_x)$ and $f(x) = 1$, respectively, (only the case with initial average momentum $p_0 = 0$ is shown). Note that we have taken a higher value for the numerical 0, given that the momentum range over which we need to integrate in Equation (21), for each value of t , is significantly more extended than with a $\cos^8(x/\Delta_x)$ function. Finally, Figure 6 compares the probability density propagating beyond the light cone for the three functions $f(x)$ we have considered in this paper (with the same initial compact support and mean momentum).

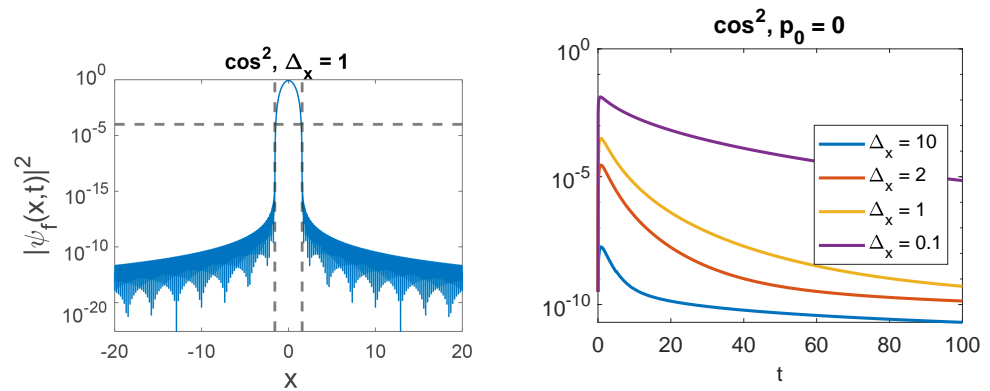


Figure 4. Left panel: $|\psi_f(t = 0, x)|^2$ is plotted in logarithmic scale for the function with compact support $f(x) = \cos^2(x/\Delta_x)$ (with $\Delta_x = 1$ and $p_0 = 0$). Right panel: fraction of the probability density leaking outside the light cone as this initial wavepacket evolves (each curve shows the result for a different width Δ_x).

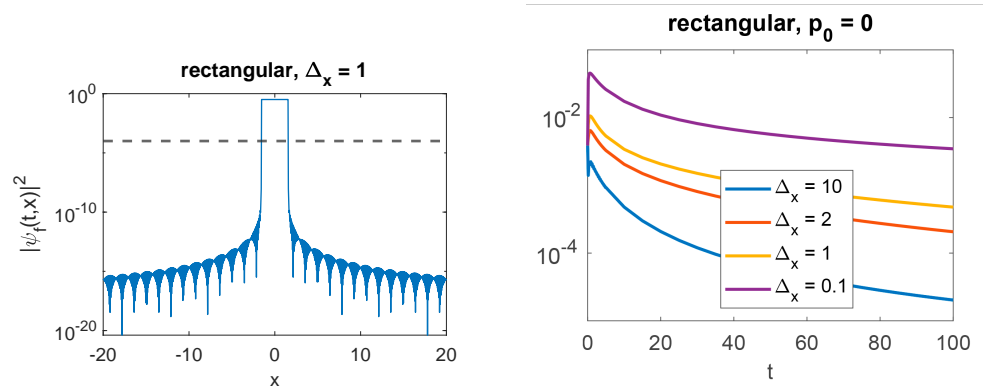


Figure 5. Same as Figure 4 but for an initial rectangle distribution, $f(x) = 1$.

We have, in addition, included two tables. Table 1 specifies the duration of significant superluminal propagation depending on $f(x)$ (the compact support) and the width. We see that in the rectangular case for a narrow wavepacket, a fraction (0.01%) of the probability density remains outside the light cone for times up to $t \approx 10^4$ in natural units (for an electron this corresponds to 1.3×10^{-17} s.). Table 2, on the other hand, is interested in short times, reporting the time at which the fraction of the probability density lying outside the light cone is maximal, as well as the value of that fraction.

Table 1. Time for which the fraction of the probability density propagating beyond the light cone remains above 10^{-4} , for different initial wavefunctions.

	$\Delta_x = 10$	$\Delta_x = 2$	$\Delta_x = 1$	$\Delta_x = 0.1$
$\cos^8, p_0 = 0$	-	-	-	$t \sim 27$
$\cos^2, p_0 = 0$	-	-	$t \sim 3.1$	$t \sim 43.5$
rectangular, $p_0 = 0$	$t \sim 225$	$t \sim 1150$	$t \sim 2250$	$t \sim 9000$

Table 2. Time for which the fraction of the probability density lying outside the light cone is maximal, along with the corresponding value of that fraction, for different initial wavefunctions (all with $p_0 = 0$).

Wavefunction	$\Delta_x = 10$	$\Delta_x = 2$	$\Delta_x = 1$	$\Delta_x = 0.1$
\cos^8	$t \sim 0.96$ 1.1×10^{-13}	$t \sim 0.89$ 2.15×10^{-6}	$t \sim 0.84$ 7.25×10^{-5}	$t \sim 0.65$ 1.38×10^{-3}
\cos^2	$t \sim 0.84$ 2.23×10^{-8}	$t \sim 0.84$ 2.88×10^{-5}	$t \sim 0.80$ 3.14×10^{-4}	$t \sim 0.66$ 1.87×10^{-3}
rectangular	$t \sim 0.64$ 2.28×10^{-3}	$t \sim 0.68$ 6.46×10^{-3}	$t \sim 0.66$ 1.06×10^{-2}	$t \sim 0.63$ 4.40×10^{-2}

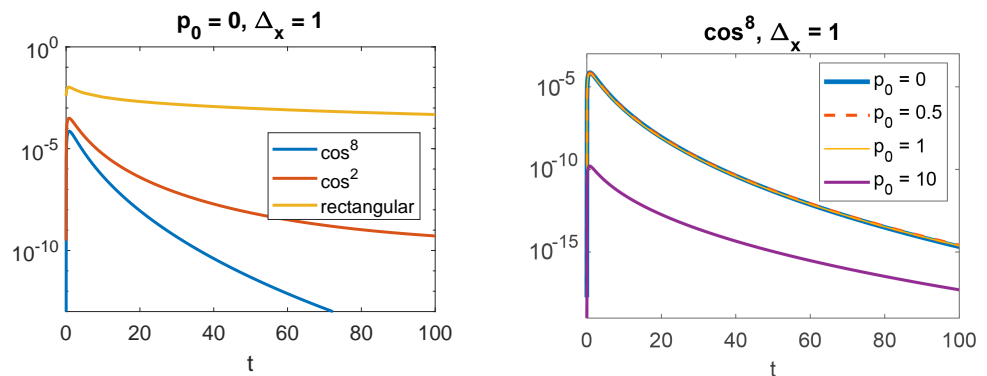


Figure 6. Fraction of the probability density leaking outside the light cone as time evolves. **Left panel:** Comparison of the three wave different initial compact supports $f(x)$ considered in this work, see Equation (19), with $p_0 = 0$ and $\Delta_x = 1$. **Right panel,** for the case $f(x) = \cos^8(x/\Delta_x)$, comparison of different values of the initial momentum p_0 (with $\Delta_x = 1$ in all cases).

5. Discussion and Conclusions

As expected from mathematical arguments, our calculations confirm that the wavefunction propagates beyond the light cone as soon as $t > 0$. Typical wavepackets will have a spatial distribution Δ_x much larger than the Compton wavelength λ_C . In this case, the propagation beyond the light cone appears as a small transient effect, though not totally negligible at short times (see the $\Delta_x = 10$ curve in Figure 5). Note that short times, of the order of $t \approx 1$ in the units used here, would lie for an electron in the zeptosecond regime, a regime that is near experimental reach [31]. Of course for heavier particles, the time scale scales inversely to the mass, so that for macroscopic bodies $t \approx 1$ would be shorter than the Planck time.

Even at considerably longer times, there is still a non-negligible probability outside the light cone (see Table 1)). For narrower wavepackets, the fraction of the probability distribution beyond the light cone can reach a non-negligible percentage (see the $\Delta_x = 0.1$ curve in Figures 3–5). While it is generally believed that the single particle formalism breaks down for wavepackets narrower than λ_C (but see [32–34]), the propagating wavepacket would still contribute to the one-particle sector of the corresponding quantum-field theoretical description [8,17]. This does not necessarily entail that the superluminal propagation could actually be detected, but, to the extent that the spatial density defined above is the correct physical one, our results indicate this possibility must be kept open.

Another interesting effect is the role of the initial average momentum. From Figure 3, one can see that the fraction of the probability density leaking beyond the light-cone decreases as p_0 increases. Somewhat paradoxically, wavepackets in the ultrarelativistic regime ($p_0 \sim 10$) remain almost entirely within the light cone, while wavepackets with initial zero momentum (whose average position does not move) are those that display the highest proportion of superluminal propagation (see Figure 6). It would be interesting to

understand the reasons for this behavior. The role of the shape of the wavepacket, which determines the range of the contributing momenta in Equation (21), is also interesting. From our choices for $f(x)$, we can say that beyond the light cone, spreading increases as the momentum range increases. Here too, there is no obvious argument to explain this behavior.

In summary, motivated by the issue of the physicality of the Foldy–Wouthuysen (FW) density, we have numerically explored the time evolution of free relativistic wavefunctions propagated by the sole positive energy propagator. We have done so by choosing three different initial wavefunctions with compact support and varying parameters. We conclude from our findings that beyond the light cone, propagation is a very small effect that is non-negligible for particles having a small mass (of the order of elementary particles) over a short time after preparation of the initial state. It is, however, impossible to assert that this effect cannot lead to any observational consequences if the FW density is taken as being the physically meaningful quantity.

Author Contributions: A.M. conceived the idea, X.G.d.l.C. wrote the codes and made the calculations, both authors prepared the draft, wrote and reviewed the manuscript. All authors have read and agreed to the published version of the manuscript.

Funding: This research received no external funding.

Informed Consent Statement: Not applicable.

Data Availability Statement: The data are contained within the article.

Conflicts of Interest: The authors declare no conflict of interest.

References

- Hegerfeldt, G.C. Instantaneous spreading and Einstein causality in quantum theory. *Ann. Phys.* **1998**, *7*, 716–725. [[CrossRef](#)]
- Kosinski, P. Salpeter Equation and Causality. *Prog. Theor. Phys.* **2012**, *128*, 59–65. [[CrossRef](#)]
- Beck, C. *Local Quantum Measurement and Relativity*; Springer Nature Switzerland: Cham, Switzerland, 2021.
- Greiner, W. *Field Quantization*; Springer: Berlin/Heidelberg, Germany, 1996.
- Padmanabhan, T. Obtaining the non-relativistic quantum mechanics from quantum field theory: Issues, folklores and facts. *Eur. Phys. J. C* **2018**, *78*, 563. [[CrossRef](#)]
- Kowalski, K.; Rembielinski, J. Salpeter equation and probability current in the relativistic Hamiltonian quantum mechanics. *Phys. Rev. A* **2011**, *84*, 012108. [[CrossRef](#)]
- Zou, L.; Zhang, P.; Silenko, A.J. Position and spin in relativistic quantum mechanics. *Phys. Rev. A* **2020**, *101*, 032117. [[CrossRef](#)]
- Pavsic, M. Localized States in Quantum Field Theory. *Adv. Appl. Clifford Algebr.* **2018**, *28*, 89. [[CrossRef](#)]
- Ruijsenaars, S.N.M. On Newton–Wigner localization and superluminal propagation speeds. *Ann. Phys.* **1981**, *137*, 33–43. [[CrossRef](#)]
- Rosenstein, B.; Usher, M. Explicit illustration of causality violation: Noncausal relativistic wave-packet evolution. *Phys. Rev. D* **1987**, *36*, 2381. [[CrossRef](#)]
- Al-Hashimi, M.H.; Wiese, U.J. Minimal position-velocity uncertainty wave packets in relativistic and non-relativistic quantum mechanics. *Ann. Phys.* **2009**, *324*, 2599–2621. [[CrossRef](#)]
- Eckstein, M.; Miller, T. Causal evolution of wave packets. *Phys. Rev. A* **2017**, *95*, 032106. [[CrossRef](#)]
- Torre, A.; Lattanzi, A.; Levi, D. Time-Dependent Free-Particle Salpeter Equation: Numerical and Asymptotic Analysis in the Light of the Fundamental Solution. *Ann. Der Phys.* **2017**, *529*, 1600231. [[CrossRef](#)]
- Greiner, W. *Relativistic Quantum Mechanics*; Springer: Berlin/Heidelberg, Germany, 1996.
- Wachter, A. *Relativistic Quantum Mechanics*; Springer: Berlin/Heidelberg, Germany, 2011.
- Salpeter, E.E. Mass Corrections to the Fine Structure of Hydrogen-Like Atoms. *Phys. Rev.* **1952**, *87*, 328. [[CrossRef](#)]
- Rosenstein, B.; Horwitz, L.P. Probability current versus charge current of a relativistic particle. *J. Phys. A Math. Gen.* **1985**, *18*, 2115. [[CrossRef](#)]
- Lucha, W.; Schoeberl, F.F. All Around the Spinless Salpeter Equation. *arXiv* **1994**, arXiv:hep-ph/9410221.
- Foldy, L.L.; Wouthuysen, S.A. On the Dirac Theory of Spin 1/2 Particles and Its Non-Relativistic Limit. *Phys. Rev.* **1950**, *78*, 29. [[CrossRef](#)]
- Case, K.M. Some Generalizations of the Foldy–Wouthuysen Transformation. *Phys. Rev.* **1954**, *95*, 1323. [[CrossRef](#)]
- Alkhateeb, M.; Matzkin, A. Relativistic Bohmian Trajectories and Klein–Gordon Currents for Spin-0 Particles. *Found. Phys.* **2022**, *52*, 104. [[CrossRef](#)]
- Redmount, I.H.; Suen, W.M. Path integration in relativistic quantum mechanics. *Int. J. Mod. Phys. A* **1993**, *8*, 1629–1635. [[CrossRef](#)]
- Newton, T.D.; Wigner, E.P. Localized States for Elementary Systems. *Rev. Mod. Phys.* **1949**, *21*, 400. [[CrossRef](#)]

24. Karpov, E.; Ordonez, G.; Petrosky, T.; Prigogine, I.; Pronko, G. Causality, delocalization, and positivity of energy. *Phys. Rev. A* **2000**, *62*, 012103. [[CrossRef](#)]
25. Pavsic, M. Manifestly covariant canonical quantization of the scalar field and particle localization. *Mod. Phys. Lett. A* **2018**, *33*, 1850114. [[CrossRef](#)]
26. Pavsic, M. A new perspective on quantum field theory revealing possible existence of another kind of fermions forming dark matter. *Int. J. Geom. Meth. Mod. Phys.* **2022**, *19*, 2250184. [[CrossRef](#)]
27. Silenko, A.J.; Zhang, P.; Zou, L. Reply to Comment on “Relativistic Quantum Dynamics of Twisted Electron Beams in Arbitrary Electric and Magnetic Fields”. *Phys. Rev. Lett.* **2019**, *122*, 159302. [[CrossRef](#)] [[PubMed](#)]
28. Gutiérrez de la Cal, X.; Alkhateeb, M.; Pons, M.; Matzkin, A.; Sokolovski, D. Klein paradox for bosons, wave packets and negative tunnelling times. *Sci. Rep.* **2020**, *10*, 19225. [[CrossRef](#)] [[PubMed](#)]
29. Alkhateeb, M.; Gutierrez de la Cal, X.; Pons, M.; Sokolovski, D.; Matzkin, A. Relativistic time-dependent quantum dynamics across supercritical barriers for Klein–Gordon and Dirac particles. *Phys. Rev. A* **2021**, *103*, 042203. [[CrossRef](#)]
30. Alkhateeb, M.; Matzkin, A. Relativistic spin-0 particle in a box: Bound states, wave packets, and the disappearance of the Klein paradox. *Am. J. Phys.* **2022**, *90*, 297. [[CrossRef](#)]
31. Mourou, G.; Mironov, S.; Khazanov, E.; Sergeev, A. Single cycle thin film compressor opening the door to Zeptosecond-Exawatt physics. *Eur. Phys. J. Spec. Top.* **2014**, *223*, 1181. [[CrossRef](#)]
32. Bakke, F.; Wergeland, H. Wave packets of relativistic electrons. *Physica* **1973**, *69*, 5–11. [[CrossRef](#)]
33. Hoffmann, S.E. The minimum width in relativistic quantum mechanics. *J. Phys. B* **2018**, *51*, 165302. [[CrossRef](#)]
34. Krekora, P.; Su, Q.; Grobe, R. Relativistic Electron Localization and the Lack of Zitterbewegung. *Phys. Rev. Lett.* **2004**, *93*, 043004. [[CrossRef](#)]

Disclaimer/Publisher’s Note: The statements, opinions and data contained in all publications are solely those of the individual author(s) and contributor(s) and not of MDPI and/or the editor(s). MDPI and/or the editor(s) disclaim responsibility for any injury to people or property resulting from any ideas, methods, instructions or products referred to in the content.